Solving the time-fractional Schrödinger equation by Krylov projection methods

Roberto Garrappa[a,*], Igor Moret[b], Marina Popolizio[c]

[a] *Università degli Studi di Bari, Dipartimento di Matematica Via E. Orabona n.4 - 70125 Bari, Italy*
[b] *Università degli Studi di Trieste, Dipartimento di Matematica e Geoscienze Via Valerio, 12/1 - 34127 Trieste, Italy*
[c] *Università del Salento, Dipartimento di Matematica e Fisica "Ennio De Giorgi" Via per Arnesano - 73100 Lecce, Italy*

Abstract

The time–fractional Schrödinger equation is a fundamental topic in physics and its numerical solution is still an open problem. Here we start from the possibility to express its solution by means of the Mittag–Leffler function; then we analyze some approaches based on the Krylov projection methods to approximate this function; their convergence properties are discussed, together with related issues. Numerical tests are presented to confirm the strength of the approach under investigation.

Keywords: time–fractional Schrödinger equation, Mittag–Leffler function, Krylov subspace methods
2000 MSC: 34A08, 65F60, 65M06, 33E12, 35Q40

1. Introduction

The time–dependent Schrödinger equation is a fundamental equation in quantum physics and describes the evolution of the position–space wave function of a particle. Its formulation dates back to 1926 by the Austrian physicist Erwin Schrödinger [1] who also laid the foundations of quantum wave mechanics.

During the last two decades a special interest has been paid to generalize some important models and equations in order to introduce derivatives of

*Corresponding author
Email addresses: roberto.garrappa@uniba.it (Roberto Garrappa), moret@units.it (Igor Moret), marina.popolizio@unisalento.it (Marina Popolizio)

fractional (i.e., non–integer) order. Experimental observations have indeed shown that the non–locality of fractional operators is a suitable tool to keep into account some anomalous phenomena and hereditary properties which can not be satisfactorily described by means of classical physical laws.

Nowadays, models based on fractional differential equations (FDEs) are commonly studied and employed in several fields, ranging from biology to engineering, finance, physics and so on (we refer, for instance, to [2–7] for an introductory overview on fractional calculus and its main applications).

The generalization to non–integer order derivatives of the Schrödinger equation has been firstly proposed by Laskin [8] who used the Feynman path integrals over the Levy trajectories to derive a space–fractional Schrödinger equation with the Laplace operator replaced by the quantum Riesz derivative. Successive contributions are due to [5, 9–13].

In [14] Naber proposed and discussed a different generalization by changing the first order time–derivative into a Caputo fractional derivative and investigated two different ways to perform this generalization, by expressing its preference on the one obtained by performing a Wick rotation.

Although the formulation of the Schrödinger equation is quite simple, finding its solutions is not in general an easy task and hence numerical approaches are often preferred in practice. However, as far as we know, very few contributions [15, 16] are available in literature on the numerical solution of the time–fractional Schrödinger equations (TFSEs).

Under a general point of view, it is well–known that classical approaches based, for instance, on finite differences are usually computationally expensive when applied to time–dependent FDEs; the presence, indeed, of a long persistent memory leads to convolution quadratures which are very demanding especially for integration over long time intervals. For these reasons, finding new and more efficient ways for numerically solving evolutionary problems of fractional order is today an active field of research.

In the recent years a considerable attention has been focused on the application of Krylov subspace methods for the approximation of the action of functions of matrices or linear operators [17–19]. This has been mainly motivated by the fact that solutions to various differential problems can be expressed in terms of such functions; on the basis of this observation, modern exponential integrators are devised (see [20] for a recent survey).

In particular for FDEs, whose solutions can be often represented through Mittag–Leffler (ML) functions, the possibility of evaluating the solution directly at some time, by means of matrix functions, appears extremely remarkable since it allows to avoid long convolution quadratures and save computational time; in this respect, we quote the recent papers [19, 21–27].

The aim of this paper is to study such approach for the numerical solution of TFSEs. For this reason we will present the standard Krylov subspace method (SKM) and we will study their convergence properties. We will also show the main problems arising in some particular situations and we will discuss some alternative strategies. In particular, the rational Arnoldi method often named as the Shift-and-Invert Krylov method (SIKM) will be here considered. Indeed, due to its good features, such procedure turns out to be particularly suited for treating various types of PDEs. In several cases, SIKM converges in a very fast way but the theoretical investigation of the convergence properties is not an easy task; this is particularly true with TFSEs whose resulting operators have the spectrum on the imaginary axis or, however, on some axis in regions affected by stability issues.

This paper is organized in the following way. In Section 2 we introduce the main formulations for the TFSEs and we provide some basis for their solution. Section 3 is devoted to present the ML function and study its main properties for operators having the same spectral location of the operators arising from spatial discretization of the TFSE. In Section 4 Krylov subspace methods are introduced and the convergence properties are investigated; since this Section is quite technical, for the sake of clearness we have moved all the proofs in an Appendix at the end of the paper. In Section 5 we present some numerical experiments and we discuss some alternative strategies in order to improve the computational efficiency.

2. Time-Fractional Schrödinger equation

The Schrödinger equation is the main tool in quantum physics to describe the position–space wavefunction $\psi = \psi(t, x)$ of a single non relativistic particle with mass $\widehat{m}$ and potential energy $V(x)$. As usual, here t denotes the independent time–variable and x the spatial coordinates in a certain domain $\Omega \subseteq \mathbb{R}^p$, $p \in \{1, 2, 3\}$. One of the simplest formulations of the time–dependent Schrödinger equation is provided by

$$i\hbar \frac{d}{dt}\psi = -\frac{\hbar^2}{2\widehat{m}}\nabla_x^2\psi + V(x)\psi,$$

where ∇_x^2 is the classical Laplacian operator with respect to the spatial variable $x \in \Omega$, $i = \sqrt{-1}$ is the imaginary unit and $\hbar$ the reduced Planck's constant. In more sophisticated quantum models, the Hamiltonian

$$H(x) = -\frac{\hbar^2}{2\widehat{m}}\nabla_x^2 + V(x)$$

is replaced by more complex operators, which possibly vary with respect to the time; however we will not address these cases and we will focus on the above basic form of $H(x)$. We recall that under suitable conditions on V (see the Kato–Rellich theorem in [28]), the operator H is self adjoint.

Substantially, the following two distinct options emerge for the generalization of the time–dependent Schrödinger equation to fractional order [14]:

$$i\hbar T_p^{\alpha-1}\, {}_0D_t^{\alpha}\psi = -\frac{\hbar^2}{2\widehat{m}}\nabla_x^2\psi + V(x)\psi \tag{1}$$

and

$$i^{\alpha}\hbar T_p^{\alpha-1}\, {}_0D_t^{\alpha}\psi = -\frac{\hbar^2}{2\widehat{m}}\nabla_x^2\psi + V(x)\psi, \tag{2}$$

where T_p denotes the Planck time; for a function u which is assumed n times differentiable in $[0, T]$ with an absolutely continuous n-th derivative, ${}_0D_t^{\alpha}u(t)$ is the Caputo's fractional derivative defined according to

$${}_0D_t^{\alpha}u(t) = \frac{1}{\Gamma(n-\alpha)}\int_0^t (t-s)^{n-1-\alpha}u^{(n)}(s)ds, \quad t \in (0, T],$$

for $n \in \mathbb{N}$, $n - 1 < \alpha < n$, and $\Gamma(z) = \int_0^{\infty} s^{z-1}e^{-s}ds$ the Euler's gamma function.

The choice to raise or not i to the order of the time derivative has physical motivations. In [14], the author motivates to choose the latter as the natural formulation of the TFSE because its solution preserves the main physical features as α moves from integer to fractional values in the neighborhood of 1. On the contrary, other authors [29] introduced some considerations supporting formulation (1). Without entering into this type of discussion, since this paper focuses on the numerical solution of the fractional Schrödinger equation, we will not express any preference for any of these formulations and we will face the numerical treatment of both cases.

Nevertheless, for the sake of completeness, we must also mention a third formulation which has been recently proposed in [30] on the basis of the same arguments (the Wick rotation and its inverse) used in [14] to derive (2). This formulation is qualitatively similar to (2) and, from the numerical point of view, does not add any supplementary difficulty with respect to (2) and therefore we will not further consider it.

To provide a concise notation we recast problems (1) and (2) in the more general framework

$${}_0D_t^{\alpha}y(t) = A_{\eta}y(t), \quad A_{\eta} = (-i)^{\eta}A \tag{3}$$

with $\eta = 1$ or $\eta = \alpha$ according to the fact that we are dealing respectively with equation (1) or (2). Here A is a suitable positive self–adjoint linear operator (not involving time differentiation) acting on a (separable) Hilbert space $\mathcal{H}$ with spectrum $\sigma(A) \subset [a, +\infty)$, with $a > 0$ and a dense domain $\mathcal{D}(A) \subseteq \mathcal{H}$.

The framework (3) is very general and allows to look at the same problem under different points of view: from an abstract perspective A denotes the infinite dimensional operator $A = T_p^{1-\alpha}\hbar^{-1}H(x)$; in a numerical setting A is a finite dimensional operator (namely a matrix) resulting from spatial discretization of $T_p^{1-\alpha}\hbar^{-1}H(x)$ (for instance, by means of finite differences, spectral methods or finite elements).

Throughout this paper we will confine our attention only to real values of α with $0 < \alpha < 1$, since this is the case of more interest in practical applications. Classical theoretical results (see e.g. [6, 7, 31]) state that when equation (3) is coupled with the initial condition $y(0) = v$ its solution can be represented as

$$y_\alpha(t) = e_{\alpha,1}(t; A_\eta)v$$

with

$$e_{\alpha,\beta}(t; z) = t^{\beta-1}E_{\alpha,\beta}(t^\alpha z) \tag{4}$$

denoting a generalization of the Mittag–Leffler (ML) function

$$E_{\alpha,\beta}(z) = \sum_{k=0}^{\infty} \frac{z^k}{\Gamma(\alpha k + \beta)}, \quad z \in \mathbb{C}. \tag{5}$$

Although it is possible to study the evaluation of ML functions on possibly unbounded operators (see e.g. [25, 26]), in practice we work in finite dimension; hence, from now on we assume that A is a real symmetric positive definite square matrix (usually arising from some suitable discretization of the continuous operator $H(x)$).

3. The Mittag–Leffler function: integral formulations and properties

The ML functions $E_{\alpha,\beta}$ and $e_{\alpha,\beta}$ play a crucial role in the analysis and solution of FDEs, including the TFSE under consideration. The investigation of some of their main properties is therefore of primary importance.

In the past several (more or less equivalent) representations of the ML function, mostly in integral form, have been proposed. The introduction of different formulations is motivated by the fact that some of them turn out to be useful for the investigation of theoretical properties whereas others are of practical utility for computation.

In this Section we briefly review some representations of the ML function in order to present the main properties which will be used in the forthcoming analysis.

3.1. Integral formulation based on the Hankel representation

One of the most used formulations was first proposed in [32] for the case $\beta = 1$, and hence in [33] for any arbitrary β, and it is based on the use of the Hankel's integral representation for the reciprocal of the Gamma function in (5). To this purpose we consider, in the complex plane, the contour $Q(\varepsilon, \mu)$, with $\alpha\frac{\pi}{2} < \mu \leq \min[\pi, \alpha\pi]$ and $\varepsilon > 0$, oriented in a counterclockwise direction and consisting of the following three parts:

1. $\arg \xi = -\mu$, $|\xi| > \varepsilon$;
2. $-\mu \leq \arg \xi \leq \mu$, $|\xi| = \varepsilon$;
3. $\arg \xi = \mu$, $|\xi| > \varepsilon$.

The contour $Q(\varepsilon, \mu)$ divides the complex plane into a left domain $G_-(\varepsilon, \mu)$ and a right domain $G_+(\varepsilon, \mu)$ as shown in Figure 1 (left plot). The choice $\mu = \pi$ is allowed when $\alpha \geq 1$ and $G_+(\varepsilon, \pi)$ becomes $\mathbb{C}$ excluding the circle $|z| < \varepsilon$ and the line $|\arg z| = \pi$ (see the right plot of Figure 1). For $t > 0$ the following representation [7, Theorem 1.1.] holds: if $z \in G_-(\varepsilon, \mu)$ then

$$e_{\alpha,\beta}(t; z) = \frac{1}{2\alpha\pi i} \int_{Q(\varepsilon,\mu)} \exp(-t\xi^{\frac{1}{\alpha}})\xi^{\frac{1-\beta}{\alpha}}(\xi - z)^{-1} d\xi \tag{6}$$

and if $z \in G_+(\varepsilon, \mu)$ then

$$e_{\alpha,\beta}(t; z) = \frac{1}{\alpha} z^{\frac{1-\beta}{\alpha}} \exp(tz^{\frac{1}{\alpha}}) + \frac{1}{2\alpha\pi i} \int_{Q(\varepsilon,\mu)} \exp(-t\xi^{\frac{1}{\alpha}})\xi^{\frac{1-\beta}{\alpha}}(\xi - z)^{-1} d\xi. \tag{7}$$

The above formulas are usually used to study the ML function (mainly to get asymptotic expansions), but they have been also employed for numerical computation (see e.g. [34, 35]).

Formulas (6) and (7) are likely to be useful since the extension to matrix arguments is straightforward, recalling that $A^{\frac{1}{\alpha}}$ can be (uniquely) defined through Schur decomposition in such a way that it is symmetric positive definite too. We point out that we are interested to give convergence results which hold for every discretization of $H(x)$. This motivates to assume that the spectrum $\sigma(A)$ is contained in $[a, +\infty)$, $a > 0$. Yet, by this fact, when

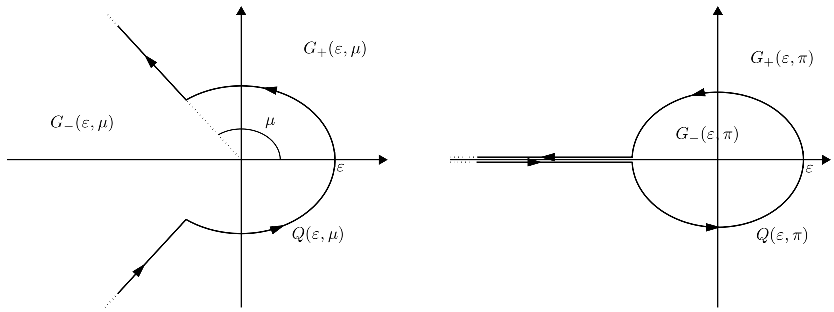

Figure 1: Contour $Q(\varepsilon, \mu)$ and left and right domains $G_-(\varepsilon, \mu)$ and $G_+(\varepsilon, \mu)$ for $\mu < \pi$ (left plot) and $\mu = \pi$ (right plot).

$\eta = \alpha$ we cannot employ formula (6) and we are compelled to use (7) with $\varepsilon < a$ in order to ensure that the whole spectrum of $(-i)^\alpha A$ is contained in $G_+(\varepsilon, \mu)$. Accordingly, referring to (3) and (4), in analyzing the proposed methods we will make use of (6) when $\eta = 1$ and of (7) when $\eta = \alpha$.

3.2. Integral formulation based on the Laplace transform

The Laplace transform of the generalized ML function $e_{\alpha,\beta}(t; z)$ is [6, 7]

$$\mathcal{E}_{\alpha,\beta}(s; z) = \mathcal{L}(e_{\alpha,\beta}(t; z)) = \frac{s^{\alpha-\beta}}{s^\alpha - z}.$$

Because of the presence of real powers, $\mathcal{E}_{\alpha,\beta}(s; \lambda)$ is a multi-valued function; to make it single-valued we thus select a branch cut from 0 to $-\infty$ along the negative real axis.

It is therefore possible to represent $e_{\alpha,\beta}(t; \lambda)$ by means of the formula for the inversion of the Laplace transform

$$e_{\alpha,\beta}(t; z) = \frac{1}{2\pi i} \int_{\mathcal{C}} e^{st} \mathcal{E}_{\alpha,\beta}(s; z) ds,$$

where $\mathcal{C}$ is a contour in the complex plane obtained by deforming the Bromwich line in a suitable way to encompass all the singularities of $\mathcal{E}_{\alpha,\beta}(s; z)$.

The contour $\mathcal{C}$ can be deformed into an Hankel contour $\mathcal{H}_\gamma$ which starts from $-\infty$, moves below the negative real semi-axis, surrounds the origin in the positive (counterclockwise) sense along a circular disc $|s| = \gamma$ and returns at $-\infty$ above the negative real semi-axis. By letting $\gamma \to 0$, the contour $\mathcal{H}_\gamma$ crosses the poles of $\mathcal{E}_{\alpha,\beta}$ which are therefore removed by residue subtraction

$$e_{\alpha,\beta}(t; z) = \sum_{s^\star \in S} Res(e^{st} \mathcal{E}_{\alpha,\beta}(s; z), s^\star) + \lim_{\gamma \to 0} \frac{1}{2\pi i} \int_{\mathcal{H}_\gamma} e^{st} \mathcal{E}_{\alpha,\beta}(s; z) ds, \quad (8)$$

where S is the set of all singularities of $\mathcal{E}_{\alpha,\beta}$ except the branch–point singularity at the origin and $Res(f, s^\star)$ denotes the residue of f at $s^\star$.

Thanks to (8) we are able to decompose $e_{\alpha,\beta}(t;z)$ into two terms

$$e_{\alpha,\beta}(t;z) = F^{(1)}_{\alpha,\beta}(t;z) + F^{(2)}_{\alpha,\beta}(t;z), \tag{9}$$

where

$$F^{(1)}_{\alpha,\beta}(t;z) = \lim_{\gamma\to 0} \frac{1}{2\pi i} \int_{\mathcal{H}_\gamma} e^{st} \mathcal{E}_{\alpha,\beta}(s;z) ds$$

and

$$F^{(2)}_{\alpha,\beta}(t;z) = \sum_{s^\star \in S} Res(e^{st}\mathcal{E}_{\alpha,\beta}(s;z), s^\star) = \frac{1}{\alpha} \sum_{s^\star \in S} e^{ts^\star} (s^\star)^{1-\beta}.$$

3.3. Behavior of $e_{\alpha,\beta}(t;z)$ for complex arguments

Splitting the ML function according to (9) can be useful for investigating some of its properties. In particular we are interested in studying the behavior of $e_{\alpha,\beta}(t;(-i)^\eta \lambda)$ for real and positive λ ranging from 0 to $+\infty$.

The completely monotonic (c.m.) character of the ML function, in the presence of real arguments, has been studied by several authors (see, for instance, [6, 36–39]). We recall that a function $f(x)$ is c.m. when $(-1)^k f^{(k)}(x) \geq 0$ for all $k = 0, 1, \ldots$ and $x > 0$. The c.m. property is of interest since it assures a high level of smoothness.

These results on the c.m. of the ML can not be directly extended to the more general case under investigation but anyway we can the same provide useful information of this kind for $F^{(1)}_{\alpha,\beta}(t;z)$.

Proposition 1. *The function $F^{(1)}_{\alpha,\beta}(t;z)$ is a linear combination of a finite number of c.m. functions.*

Proof. By letting $\gamma \to 0$, the Hankel's path $\mathcal{H}_\gamma$ collapses onto the branch cut and it is an elementary task to verify, after standard manipulations, that $F^{(1)}_{\alpha,\beta}(t;z)$ can be equivalently written as

$$\begin{aligned} F^{(1)}_{\alpha,\beta}(t;z) &= \frac{1}{2\pi i} \int_0^\infty e^{-rt} r^{\alpha-\beta} \frac{r^\alpha e^{i\beta\pi} - \bar{z} e^{-i(\alpha-\beta)\pi}}{r^{2\alpha} - 2r^\alpha \Phi_\alpha(\bar{z}) + |z|^2} dr - \\ & \frac{1}{2\pi i} \int_0^\infty e^{-rt} r^{\alpha-\beta} \frac{r^\alpha e^{-i\beta\pi} - \bar{z} e^{i(\alpha-\beta)\pi}}{r^{2\alpha} - 2r^\alpha \Phi_\alpha(z) + |z|^2} dr, \end{aligned}$$

where $\Phi_\alpha(z) : \mathbb{C} \to \mathbb{R}$ denotes the real–valued function defined according to $\Phi_\alpha(z) = \Re(z) \cos\alpha\pi + \Im(z) \sin\alpha\pi$. Therefore, if we introduce the functions

$$G_{\alpha,\beta}(t;z) = \int_0^{+\infty} e^{-rt} K_{\alpha,\beta}(r;z) dr, \quad K_{\alpha,\beta}(r;z) = \frac{r^{\alpha-\beta}}{r^{2\alpha} - 2r^\alpha \Phi_\alpha(z) + |z|^2}$$

we are able to express $F^{(1)}_{\alpha,\beta}(t;z)$ as the linear combination

$$\begin{aligned} F^{(1)}_{\alpha,\beta}(t;z) &= \frac{e^{i\beta\pi}}{2\pi i} G_{\alpha,\beta-\alpha}(t;\bar{z}) - \frac{e^{-i\beta\pi}}{2\pi i} G_{\alpha,\beta-\alpha}(t;z) \\ &\quad - \frac{\bar{z}e^{-i(\alpha-\beta)\pi}}{2\pi i} G_{\alpha,\beta}(t;\bar{z}) + \frac{\bar{z}e^{i(\alpha-\beta)\pi}}{2\pi i} G_{\alpha,\beta}(t;z) \end{aligned}$$

(observe that although very similar, here with $K_{\alpha,\beta}(r;z)$ we denote a slightly different function with respect to the spectral function denoted by the same symbol in other papers, for instance [6, 36, 40]).

Since $\Phi_\alpha(z) = |z|\cos(\theta - \alpha\pi)$, with $\theta = \arg z$, it is $K_{\alpha,\beta}(r;z) \geq 0$ for any $0 \leq r < +\infty$. Hence, thanks to the Bernstein's theorem, the real–valued function $G_{\alpha,\beta}(t;z)$ is c.m., thus concluding the proof. □

Proposition 1 is not sufficient to guarantee that $F^{(1)}_{\alpha,\beta}(t;z)$ is c.m. too (to obtain this result the coefficients in the linear combination should be non negative) but it allows to state that it is infinitely time differentiable for $t > 0$. Moreover, since $F^{(1)}_{\alpha,\beta}(t;z)$ is a linear combination of a finite number of monotonic functions, it is expected to have a quite smooth behavior; the sign of its derivative can indeed change a (very small) finite number of times and hence we can exclude the presence of oscillations. A graphical analysis allows to better understand the smooth character of this function for $\beta = 1$ (although the behavior of the ML function is usually investigated with respect to the independent variable t, with z playing the role of a fixed argument, when $z = (-i)^\eta\lambda$, with $\lambda > 0$, the roles of t and λ can be easily swapped since $e_{\alpha,1}(t;(-i)^\eta\lambda) = e_{\alpha,1}(\lambda^{1/\alpha};(-i)^\eta t^\alpha)$).

Albeit $F^{(1)}_{\alpha,1}(t;(-i)^\eta\lambda)$ is non monotonic, both its real and imaginary parts turn out to be bounded for $0 < \lambda < +\infty$ and asymptotically they tend to 0 as $\lambda \to \infty$; we can observe this behavior in Figure 2, where for $t = 1$ we plotted $F^{(1)}_{\alpha,1}(t;-i\lambda)$ for some instances of α, and in Figure 3, where the same plots are presented for $\eta = \alpha$. In both cases, the absence of repeated oscillations suggests a certain level of smoothness which facilitates the numerical approximation on matrix arguments by means of Krylov subspace, as we will better observe later on.

To study the second term $F^{(2)}_{\alpha,1}(t;(-i)^\eta\lambda)$ it is preliminarily necessary to establish the number and the location of the poles of $\mathcal{E}_{\alpha,1}(s;(-i)^\eta\lambda)$.

Since $\lambda > 0$ is real, the possible roots of $s^\alpha - (-i)^\eta\lambda = 0$ are clearly

$$s^\star_j = ((-i)^\eta\lambda)^{1/\alpha} = \lambda^{1/\alpha} e^{i\frac{(4j-\eta)}{2\alpha}\pi}, \quad j \in \mathbb{Z}.$$

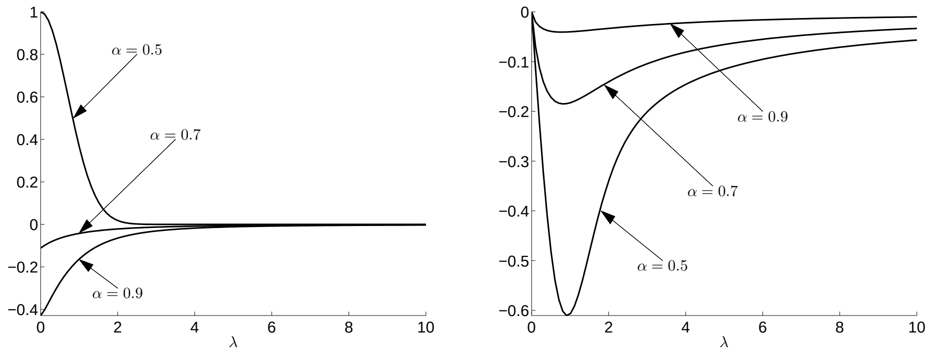

Figure 2: Plots of $F^{(1)}_{\alpha,1}(t;-i\lambda)$ for real $\lambda > 0$ and $t = 1$. The real part is in the left plot and the imaginary part in the right plot.

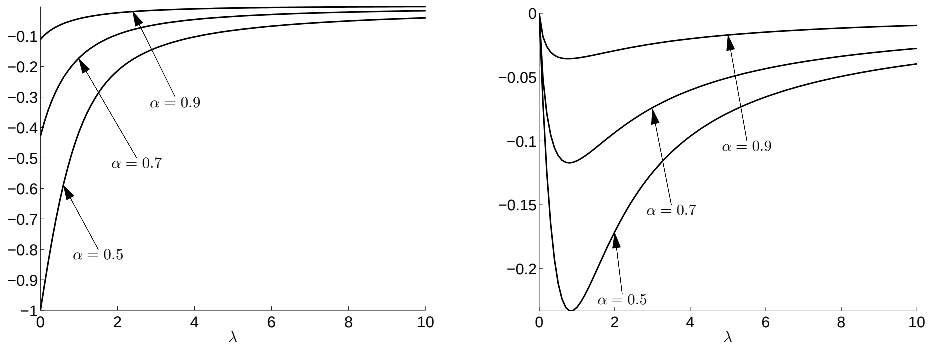

Figure 3: Plots of $F^{(1)}_{\alpha,1}(t;(-i)^{\alpha}\lambda)$ for real $\lambda > 0$ and $t = 1$. The real part is in the left plot and the imaginary part in the right plot.

Only the poles in the main Riemann sheet are relevant, i.e. the poles with the argument in $(-\pi, \pi]$.

In the case $\eta = 1$, it is immediate to verify that there are no relevant poles when $0 < \alpha \le 1/2$ while, when $1/2 < \alpha \le 1$, one pole $s^{\star} = \lambda^{1/\alpha} e^{-i\frac{\pi}{2\alpha}}$ exists. The function $F^{(2)}_{\alpha,1}(t;-i\lambda)$ thus vanishes for $0 < \alpha \le \frac{1}{2}$ while, for $\frac{1}{2} < \alpha < 1$, we can reformulate $F^{(2)}_{\alpha,1}(t;-i\lambda)$ as

$$F^{(2)}_{\alpha,1}(t;-i\lambda) = \frac{1}{\alpha} e^{\phi_\alpha t \lambda^{1/\alpha}}$$

with $\phi_\alpha = e^{-i\frac{\pi}{2\alpha}}$. Since ϕ_α lies in the third quadrant of the complex plane, the function $F^{(2)}_{\alpha,1}(t;-i\lambda)$ presents damped oscillations as λ increases in $[0, +\infty)$. The whole function $e_{\alpha,1}(t;-i\lambda)$ is therefore the sum of a rapidly decaying term $F^{(1)}_{\alpha,1}(t;-i\lambda)$ and a term $F^{(2)}_{\alpha,1}(t;-i\lambda)$ whose oscillations decay faster as α becomes smaller, until they completely vanish for $\alpha < 1/2$.

For $\eta = \alpha$ there is just one relevant pole $s^\star = -\lambda^{1/\alpha} i$. We can therefore reformulate $F^{(2)}_{\alpha,1}(t;(-i)^\alpha\lambda)$ as

$$F^{(2)}_{\alpha,1}(t;(-i)^\alpha\lambda) = \frac{1}{\alpha} e^{-it\lambda^{1/\alpha}}.$$

The presence of the term $e^{-it\lambda^{1/\alpha}}$ indicates the oscillating character of $F^{(2)}_{\alpha,1}(t;(-i)^\alpha\lambda)$ which never decays. The frequency of the oscillations can be high according to the value of λ and, as we will observe in the numerical tests of Section 5, this can create some convergence problems when the ML function has to be evaluated on matrices with a large spectrum.

4. Krylov projection methods

Approximating the value of a function with matrix argument (or the action of a matrix function on a given vector) is, in general, a complex task. Several approaches have been studied in the past and their effectiveness strictly depend on the specific properties of the function and the matrix. Thus, as pointed out in [41], where a detailed account of the main methods available for the computation of matrix exponentials is provided, it is not possible to conclude the superiority of a method over the others.

When the matrix A has small dimensions the computation of $e_{\alpha,1}(t, A_\eta)v$ can be carried out by employing Schur diagonalization, provided that a suitable code for the computation of scalar ML functions is at disposal. When A is large, as it usually occurs with discretized differential operators, Schur decomposition may be unfeasible. A remedy which is usually adopted in approximating the action of matrix functions consists in reducing the dimension of the problem by the use of Krylov projection methods.

Krylov subspace methods are indeed particularly effective for large and very large size problems and they have recently gained an increasing attention so as to be included as the twentieth approach among the "nineteen ways" for evaluating the exponential matrix in the updated review [42].

Let us consider the general problem of computing $f(A)w$, where f and w are given function and vector respectively and A a real matrix argument. Let $\mathbb{K}$ be a subspace of $\mathbb{C}^N$ and let the projection $P : \mathbb{C}^N \to \mathbb{K}$ be orthogonal. Then let $\overline{A}$ be the restriction to $\mathbb{K}$ of PA, namely

$$\overline{A} = PA : \mathbb{K} \to \mathbb{K}. \tag{10}$$

Clearly $\overline{A}$ is real, positive and self–adjoint too with $\sigma(\overline{A}) \subset [a, +\infty)$. Then we approximate $f(A)w$ by $f(\overline{A})Pw$, with $\mathbb{K}$ taken as a suitable Krylov subspace.

From now on let Π_k denote the set of the algebraic polynomials of degree equal or less than k. As usual, given a matrix M and a vector w we indicate by $K_{k+1}(M, w) = \{p(M)w, p \in \Pi_k\}$, $k = 0, 1, 2, \ldots$, the k-th Krylov subspace generated by M and w. As already mentioned, in this paper we focus the attention on the so-called Shift-and-Invert Krylov method (SIKM) where the Krylov subspaces are generated by the matrix

$$Z = (\delta I + A)^{-1}$$

for a suitably chosen real scalar $\delta > 0$ and I the identity matrix. Accordingly, one-pole rational approximations are produced.

A further motivation for considering A as a matrix, instead of an abstract operator, is that we are allowed to make comparisons with the SKM; indeed, since with the SKM the subspaces are generated by A, polynomial approximations are produced thus demanding for an high level of smoothness which is, in general, quite difficult to guarantee with abstract operators.

The results of our analysis, reported in the following subsections, will explain the convergence features of both methods when applied to the computation of $e_{\alpha,1}(t, A_\eta)v$.

Let us denote by W a matrix whose columns are an orthonormal basis of $\mathbb{K}$. Its computation can be provided by the standard Lanczos algorithm. Thus we have $P = WW^*$, where W^* denotes the adjoint of W. Accordingly let us consider the self–adjoint matrix W^*AW and its Schur decomposition $W^*AW = Q^*DQ$. Therefore $f(\overline{A})Pw$ can be approximated as $WQ^*f(D)QW^*w$.

Since in practice the matrix W^*AW is of reduced dimension, its Schur decomposition is not particularly expensive and only the evaluation of the ML function with scalar arguments is hence required. We point out that, implementing the Krylov projection in the above way, the subspaces are constructed handling real matrices and complex arithmetic is (possibly) involved only in the evaluation of scalar ML functions.

4.1. Convergence results

Here and in the sequel C will denote any generic constant independent of A as well as of all the involved parameters. The norm introduced, both for vectors and matrices, is the hermitian one.

Since, as it appears in the literature, the TFSEs arising in the practice concern values of α close to 1, here we restrict the analysis to the interval

$\frac{1}{2} < \alpha \leq 1$. In the convergence analysis we distinguish the various cases, considering both the SIKM and the SKM. The proofs of the propositions below are reported in the Appendix.

4.2. The case of the TFSE (1), i.e. $\eta = 1$

Given a vector v, we denote with $\overline{y}_\alpha(t)$ the approximation

$$\overline{y}_\alpha(t) = e_{\alpha,1}(t; -i\overline{A})Pv$$

to the solution to the TFSE (3) where, referring to (10), we first consider the SIKM (see Proposition 2) and hence the SKM (see Proposition 3). The statements below cover even the case of the standard Schrödinger equation (i.e., $\alpha = 1$). For any $\alpha < 1$ we put for shortness

$$\mu = \frac{(1+\alpha)\pi}{4}, \quad \widetilde{\omega} = \frac{1 + \sqrt{1 + (\tan\mu)^2}}{\sqrt{1 + (\tan\mu + 1)^2}}.$$

Proposition 2. *Let $\frac{1}{2} < \alpha < 1$ and $\mathbb{K} = K_{m+1}(Z, v)$, for $m \geq 1$ and $\delta > 0$. Then, for any $t > 0$,*

$$\|y_\alpha(t) - \overline{y}_\alpha(t)\| \leq C\frac{\|Av\|}{\delta}\left[\exp(t\delta^{\frac{1}{\alpha}})q^m + \sqrt{\cos\mu}\exp\left(-\frac{f(r_m)}{2}\right)\right], \quad (11)$$

where f denotes the function $f(r) = 2t(\delta r)^{\frac{1}{\alpha}}\left|\cos(\mu/\alpha)\right| + r^{-\frac{1}{2}}m\cos\mu$ and

$$q = \frac{1}{\widetilde{\omega} + \sqrt{\widetilde{\omega} - 1}}, \quad r_m = \max\left[\left(\frac{\alpha m\cos\mu}{2t\delta^{\frac{1}{\alpha}}\left|\cos\frac{\mu}{\alpha}\right|}\right)^{\frac{2\alpha}{\alpha+2}}, \frac{1}{\cos\mu}\right].$$

Moreover we have

$$\limsup_{\alpha\to 1}\|y_\alpha(t) - \overline{y}_\alpha(t)\| \leq C\frac{\exp(t\delta^{\frac{1}{\alpha}})\,\|Av\|}{\delta}(\bar{q}^m + m^{-\frac{1}{3}}), \quad (12)$$

where $\bar{q} = \sqrt{5}/(1 + \sqrt{2} + \sqrt{2(\sqrt{2} - 1)})$.

Proposition 3. *Let $\frac{1}{2} < \alpha \leq 1$ and $\mathbb{K} = K_m(A, v)$, for $m \geq 1$. Then, for any $t > 0$,*

$$\|y_\alpha(t) - \overline{y}_\alpha(t)\| \leq C\frac{\|(t^\alpha A)^m v\|}{(\alpha m)^{\alpha m}}\exp(\alpha m). \quad (13)$$

Proposition 2 shows that the rate of convergence (i.e., the error's decay with respect to m) of the SIKM is actually independent of A, even if the error bounds depend on $\|Av\|$. Accordingly, to extend the results to an unbounded operator A in (3) it is necessary to assume that $v \in \mathbb{D}(A)$.

In order to choose δ, one could minimize the error bounds. More simply, the bounds suggest that, for all t, say in the interval $(0, T]$, something like $\delta = \frac{1}{T^\alpha}$ should be a reasonable choice (we also refer the reader to our numerical experiments).

On the other hand, Proposition 3 shows that the rate of convergence of the SKM depends strongly on A and even if a superlinear convergence is eventually achieved, this may occur only for very large values of m. This fact was already pointed out in the literature devoted to the numerical treatment of the classical (i.e., $\alpha = 1$) Schrödinger equation (see e.g. [43, 44])

Obviously, in order to apply the bound (13) to an abstract operator in (3) we must assume $v \in \mathbb{D}(A^m)$.

We also notice that, by some slight changes in the proofs, it is possible to obtain similar bounds also for $0 < \alpha \leq \frac{1}{2}$.

4.3. The case of the TFSE (2), i.e. $\eta = \alpha$

As we expected, this case turns out to be more difficult to be handled, since the spectrum of $(-i)^\alpha A$ lies on the border of the stability region $\left\{|\arg(\lambda)| \geq \alpha \frac{\pi}{2}\right\}$. As previously pointed out, in this case $e_{\alpha,1}(t, (-i)^\alpha A)$ will be expressed through formula (7) with $\varepsilon < a$. For our purposes we will treat the two components of (7) separately.

In order to analyze the SKM (see Propositions 5 and 7) we need now to set an upper bound on $\sigma(A)$; in this way the role of the conditioning of A can be pointed out.

We begin with the computation of

$$w_\alpha(t) = \frac{\exp(-itA^{\frac{1}{\alpha}})}{\alpha} v.$$

Dealing with the SIKM it is convenient to rewrite $w_\alpha(t)$ as $w_\alpha(t) = g(A)Av$, where $g(z) = \exp(-itz^{1/\alpha})z^{-1}/\alpha$. Accordingly, we approximate $w_\alpha(t)$ by $\overline{w}_\alpha(t) = g(\overline{A})Av$.

Proposition 4. *Let $\frac{1}{2} < \alpha < 1$ and $\mathbb{K} = K_{m+1}(Z, Av)$, for $m \geq 1$ and $\delta = a$. Then, for any $t > 0$,*

$$\|w_\alpha(t) - \overline{w}_\alpha(t))\| \leq C \frac{\|A^2 v\|}{a^2} \exp\left(t \frac{\pi}{3} a^{\frac{1}{\alpha}}\right) \left(3^{-m} + \left(\frac{4}{m}\right)^{\frac{2(2\alpha-1)}{\alpha+2}}\right). \quad (14)$$

When the SKM is employed, the approximation in $\mathbb{K} = K_{m+2}(A,v)$, $m \geq 0$, for $w_\alpha(t)$ is obtained by means of $\overline{w}_\alpha(t) = \exp(-it\overline{A}^{\frac{1}{\alpha}})v/\alpha$.

Proposition 5. *Let $\frac{1}{2} < \alpha < 1$ and $\mathbb{K} = K_{m+2}(A,v)$, for $m \geq 0$. Assume that $\sigma(A) \subset [a,b]$ and set $R = (b-a)/a$. Then, for any $t > 0$,*

$$\|w_\alpha(t) - \overline{w}_\alpha(t)\| \leq C\frac{\|A^2 v\|}{a^2} \exp\left(t\frac{\pi}{3}a^{\frac{1}{\alpha}}\right)\left(\exp\left(-m\sqrt{\frac{2}{R}}\right) + \left(\frac{\sqrt{2R}}{m}\right)^{\frac{2(2\alpha-1)}{2-\alpha}}\right).$$

Finally, for $\frac{1}{2} < \alpha < 1$, we consider the second term in (7)

$$u_\alpha(t) = \frac{1}{2\alpha\pi i}\int_{Q(\varepsilon,\mu)} \exp(-it\lambda^{\frac{1}{\alpha}})\,(\lambda I - (-i)^\alpha A)^{-1}\, v d\lambda$$

and the corresponding approximation

$$\overline{u}_\alpha(t) = \frac{1}{2\alpha\pi i}\int_{Q(\varepsilon,\mu)} \exp(-it\lambda^{\frac{1}{\alpha}})\left(\lambda I - (-i)^\alpha \overline{A}\right)^{-1} v d\lambda.$$

Proposition 6. *Let $\frac{1}{2} < \alpha < 1$ and $\mathbb{K} = K_{m+1}(Z,v)$, for $m \geq 1$ and $\delta = a$. Then, for any $t > 0$,*

$$\|u_\alpha(t) - \overline{u}_\alpha(t)\| \leq C\frac{\|Av\|}{a}\exp\left(t\left(\frac{a}{2}\right)^{\frac{1}{\alpha}}\right)\left(3^{-m} + \exp(-f(r_m))\right),$$

where, for $r \geq 1/2$, f defines the function $f(r) = t(ar)^{\frac{1}{\alpha}} + mr^{-1}/8$ and

$$r_m = \max\left[\left(\frac{\alpha m}{8ta^{\frac{1}{\alpha}}}\right)^{\frac{\alpha}{\alpha+1}}, \frac{1}{2}\right].$$

Proposition 7. *Let $\frac{1}{2} < \alpha < 1$ and $\mathbb{K} = K_{m+1}(A,v)$, for $m \geq 0$. Assume that $\sigma(A) \subset [a,b]$ and set $R = (b-a)/a$. Then, for any $t > 0$,*

$$\|u_\alpha(t) - \overline{u}_\alpha(t)\| \leq C\frac{\|Av\|}{a}\exp\left(t\left(\frac{a}{2}\right)^{\frac{1}{\alpha}}\right)\exp\left(-m\sqrt{\frac{2}{R}}\right).$$

Concerning the SKM, which in general can be defined only in the matrix case, Propositions 5 and 7 point out that the convergence may dramatically depend on the conditioning of A, whilst in the case of the SIKM it is again independent of A, even if the bounds depend on $\|A^2 v\|$ and on $\|Av\|$ (see Propositions 4 and 6).

If we look to A as the abstract operator in (3), the corresponding regularity conditions on the data, namely $v \in \mathbb{D}(A^2)$ and $v \in \mathbb{D}(A)$, have to be assumed.

Error bounds like (14) can be proved also for $0 < \alpha \leq \frac{1}{2}$. Their proof needs however further technicalities and we do not report them here; we plan to discuss on these points in a forthcoming paper. We just note here that, if $\frac{1}{k} < \alpha \leq \frac{1}{k-1}$, for some $k \geq 2$, then we must assume that $v \in \mathbb{D}(A^k)$ in the case of abstract operators.

5. Numerical experiments

For the numerical tests we consider a dimensionless system (i.e., $\hbar = \widehat{m} = T_p = 1$) in a finite potential well which is null in a subdomain $\Omega_p \subset \Omega$ and rises abruptly to a certain value $V_0 > 0$ outside and on the boundary of Ω_p. From a formal point of view it is

$$V(x) = \begin{cases} 0 & x \in int(\Omega_p) \\ \\ V_0 & x \in cl(\Omega \backslash \Omega_p) \end{cases}$$

where $int(\Omega_p)$ is the interior of Ω_p and $cl(\Omega \backslash \Omega_p)$ the closure of $\Omega \backslash \Omega_p$. A Gaussian initial distribution $\psi(0, x) = e^{-|x|^2/(2L^2)}$ is assumed at $t = 0$.

We restrict ourself to a 2-dimensional square domain $\Omega = (-2L, 2L) \times (-2L, 2L)$ with a square well $\Omega_p = [-L, L] \times [-L, L]$.

We perform a spatial discretization of the Laplacian ∇_x^2 by means of standard central differences on some mesh–grids, which we assume equispaced along both dimensions of Ω. The values $L = 1$ and $V_0 = 10$ are assumed in all the experiments.

All the forthcoming experiments are carried out in Matlab, version 7.9.0.529, on a computer equipped with the Intel Dual Core E5400 processor running at 2.70 GHz under the Windows XP operating system.

To evaluate the ML function on matrix arguments we use a suitably modified version of the algorithm presented in [45] (based on the numerical inversion of the Laplace transform) extended to matrix arguments via Schur decomposition.

5.1. Comparison of convergence between polynomial and rational Krylov methods

To compare the convergence behavior of the SKM with that of the SIKM (for clarity denoted respectively as *polynomial* and *rational* Krylov methods), we introduce a discretization with 50×50 grid–points, thus generating a system with a 5-point stencil of size $N = 2,500$.

The computation of $e_{\alpha,1}(t;(-i)^\eta A)v$ at some time t is performed for $\eta = 1$ and $\eta = \alpha$ until a very small error is achieved or the maximum number of 200 iterations is reached. For the fractional orders $\alpha = 0.7$ and $\alpha = 0.9$, the error, with respect to a reference solution, is hence plotted against the number of iterations (i.e., the size of Krylov subspace).

For $\eta = 1$, i.e. for the TFSE (1), the results are shown in Figure 4 for $t = 1$ (left plot) and for $t = 10$ (right plot). Bullet symbols are used to denote the error obtained with the polynomial Krylov method while diamonds denote the outcomes of the rational Krylov method. Different values of the order α are identified by means of white and black colors according to the legend in the corresponding plot.

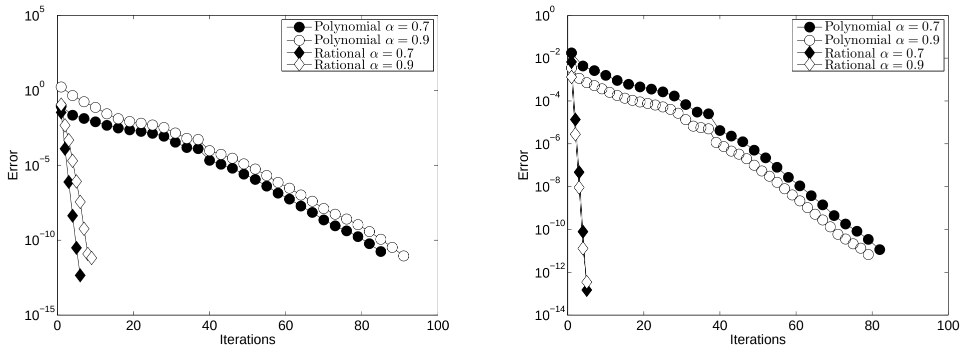

Figure 4: Errors in $e_{\alpha,1}(t;-iA)v$ by polynomial and rational Krylov methods for the 2D problem ($N = 2,500$) at $t = 1$ (left plot) and $t = 10$ (right plot).

As we can clearly see, the plots in Figure 4 are in a satisfactory agreement with the results from the theoretical investigation in Section 4. The rational Krylov method converges in a definitely faster way with respect to the polynomial counterpart. As we can see, projection onto a subspace of very reasonable dimension (namely less than 10) is sufficient to provide an accurate approximation with an error close to the precision machine; in this case the solution of the TFSE is expected to be affected fairly by just the error in the spatial discretization.

In all the above experiments the same value $\delta = 0.5$ has been used in the rational Krylov method. As discussed in [19, 46], a suitable selection of the parameter δ can accelerate the convergence. Anyway, since accurate enough results are obtained with a very small number of iterations, we think that a further investigation of optimal values for δ can be unnecessary in this case.

When the formulation (2) of the TFSE is considered, and hence $\eta = \alpha$, a more complicated situation is involved. As we can see from the error plots in Figures 5, the convergence is very slow both for the polynomial and the rational method.

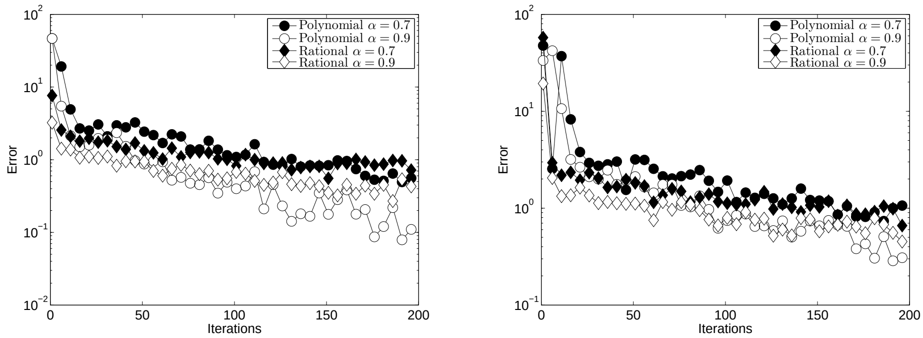

Figure 5: Errors in $e_{\alpha,1}(t;(-i)^{\alpha}A)v$ by polynomial and rational Krylov methods for the 2D problem ($N = 2,500$) at $t = 1$ (left plot) and $t = 10$ (right plot).

This bad performance is mainly due to the highly oscillating character of the ML function in $z = (-i)^{\alpha}\lambda$, as it can be inferred from the analysis in Section 3, and in particular to the presence of the oscillating and non vanishing term $F^{(2)}_{\alpha,1}(t;(-i)^{\alpha}\lambda)$.

Since the operator A resulting from the discretization of the Hamiltonian $H(x)$ has eigenvalues with large modulus (especially when a fine spatial mesh–grid is used), there result very high frequency oscillations which are badly approximated both by polynomials and rational functions. Conversely, in the case $\eta = 1$ large eigenvalues are damped in a fast way and this is the reason for the appreciable results with the TFSE (1).

5.2. An alternative approach

The above discussion on the fast converge of Krylov subspace methods when $\eta = 1$ but not when $\eta = \alpha$ suggests an alternative approach in order to overcome some of these difficulties.

According to the analysis carried out in Subsection 3.3, and in particular by applying (9) to matrix arguments, the solution $y_{\alpha}(t) = e_{\alpha,1}(t;(-i)^{\alpha}A)v$ of the TFSE can be split into the two components

$$y_{\alpha}(t) = \widehat{y}_{\alpha}(t) + \widetilde{y}_{\alpha}(t), \quad \widehat{y}_{\alpha}(t) = F^{(1)}_{\alpha,1}(t;(-i)^{\alpha}A)v, \quad \widetilde{y}_{\alpha}(t) = \frac{1}{\alpha}e^{-itA^{1/\alpha}}v.$$

Since the smooth behavior of the function $F^{(1)}_{\alpha,1}$, the approximation of $\widehat{y}_{\alpha}(t)$ by means of Krylov subspace methods does not pose any particular difficulty. Indeed, convergence of polynomial and rational Krylov methods for the case $\eta = \alpha$ is as fast as the convergence for $e_{\alpha,1}(t; -iA)$, as we can observe in Figure 6 (the same value $\delta = 0.5$ has been used).

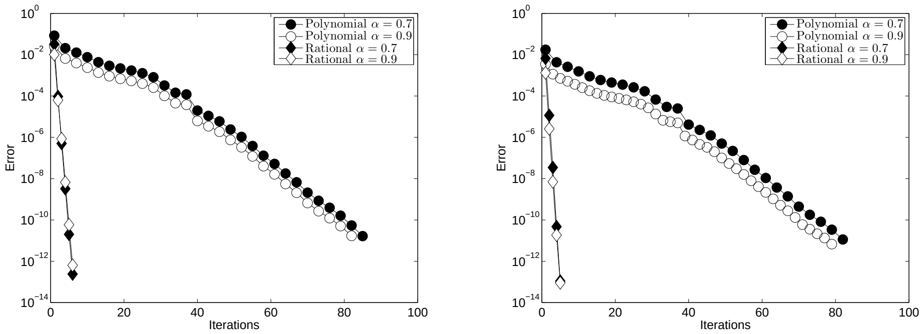

Figure 6: Error of polynomial and rational Krylov methods for $F^{(1)}_{\alpha,1}(t; (-i)^{\alpha} A^{1/\alpha})v$ for the 2D problem (N=2500) at $t = 1.0$ (left plot) and $t = 10.0$ (right plot).

The evaluation of the term $\widetilde{y}_{\alpha}(t)$ is more difficult for the presence of high frequency oscillation modes. In particular, when a large or moderately large time t is requested, both the polynomial and rational approximations of Krylov subspace methods are no more suitable to provide accurate approximations and the resulting convergence is extremely slow.

Since $\widetilde{y}_{\alpha}(t)$ is the solution of an integer–order ordinary differential equation (ODE), the use of some suitable method for oscillating ODEs can be particularly attractive in this case. We must however observe that the preliminary evaluation of $A^{\frac{1}{\alpha}}$, which can be performed by methods based on the Schur decomposition [47, 48] or contour integrals [49, 50], can be prohibitively expensive with matrices of large size.

In the presence of large size problems, it can be preferable to exploit the semigroup property of the exponential and evaluate $\widetilde{y}_{\alpha}(t)$ with Krylov subspace methods in a step-by-step fashion, as

$$\widetilde{y}_{n+1} = e^{-ihA^{1/\alpha}} \widetilde{y}_n, \quad \widetilde{y}_0 = \frac{1}{\alpha} v.$$

Once the matrix A has been projected into a suitable Krylov subspace, only the action on the vectors $\widetilde{y}_n$ of the function $\exp(-ihx^{1/\alpha})$ with a matrix argument of small size is required, thus to streamline the procedure. Indeed, by considering a sufficiently small step–size h, the frequency of the oscillations is reduced and hence it is possible to obtain a relatively fast convergence, resulting in the use of a small Krylov subspace.

Preliminary tests on this procedure seem to confirm its value especially when a moderate step–size is selected; as we can observe from Figure 7 an accuracy of 10^{-6} (smaller than the error introduced by the spatial discretization) is achieved by subspaces of moderately small size as compared to the dimension $N = 2,500$ of the problem. As expected, convergence degrades when the order α decreases since the width of the spectrum of the operator $A^{1/\alpha}$ increases. At the same time, an acceleration of the convergence is appreciated with the reduction of the step–size, due to the reduced frequency of the oscillations in the exponential.

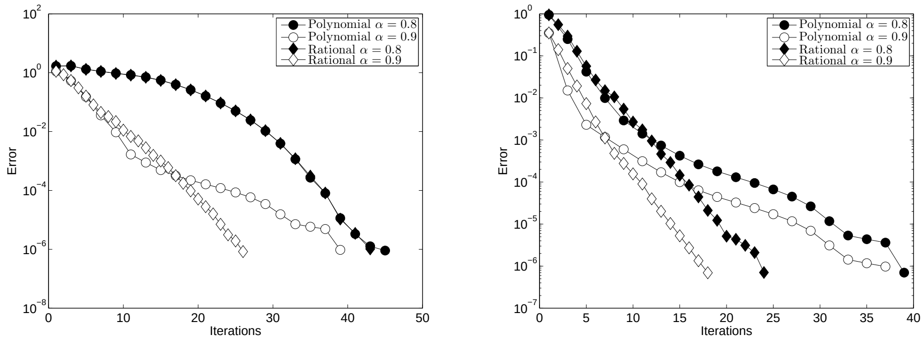

Figure 7: Error of polynomial and rational Krylov methods for $\exp(-ihA^{1/\alpha})v$ for the 2D problem (N=2500) at $h = 0.0005$ (left plot) and $h = 0.0001$ (right plot).

We are however aware that some aspects deserve a deep analysis, like the possibility to build in an effective way the spaces $K_m(A, y_n)$ or $K_m((\delta I + A)^{-1}, \widetilde{y}_n)$, the optimal balance between step–size and dimension of the Krylov subspace as well as developing a posteriori–error estimates. Our experimental observations have moreover shown that an accurate choice of the shift parameter δ can be of great help to improve efficiency (in the tests of Figure 7 we selected, on an experimental basis, the values $\delta = 200,000$ and $\delta = 4,000$ respectively for $\alpha = 0.8$ and $\alpha = 0.9$ with $h = 0.0005$ and the values $\delta = 5,000$ and $\delta = 2,000$ for $h = 0.0001$).

Motivated by these observations and by the fact that the numerical computation of $\exp(-itA^{1/\alpha})$ is inherently an interesting topic, we intend to devote a forthcoming paper to this subject.

We just remark here the possibility of splitting the original problem in two subproblems: the first of fractional nature and still suffering from *memory issues* but which can be easily solved by means of Krylov subspace methods; the latter of integer order, and hence with a *memory–free* character, but whose difficulties are related to the oscillating nature. We think that new scenarios open up for the development of new and alternative strategies in which different approaches are used to handle with the particular nature and difficulties of each subproblem.

Acknowledgements

The authors are grateful to the anonymous reviewers for their valuable comments which allowed to improve the quality of the paper.

The work of R.Garrappa and M.Popolizio is supported under the INdAM–GNCS Project 2014. The work of I.Moret is supported by Università degli Studi di Trieste under the grant "Finanziamento di Ateneo per progetti di ricerca scientifica – FRA 2013".

Appendix A. Proofs of the convergence properties

In this Appendix we collect the proofs of the propositions presented in Section 4 together with some preliminary results.

From now on, for $\xi(\neq 0) \notin [a, +\infty)$, we set

$$D(\xi) = (\xi I - A)^{-1} - (\xi I - \overline{A})^{-1} P. \tag{A.1}$$

The following lemmas hold in the light of the identity

$$D(\xi)(\xi I - A)b = 0, \qquad \text{for } b \in \mathbb{K}. \tag{A.2}$$

Lemma 8. *Let* $\mathbb{K} = K_k(A, w)$*, for* $k \geq 0$*. Then for every* $p_k \in \Pi_k$ *it is*

$$D(\xi)w = D(\xi)\frac{p_k(A)w}{p_k(\xi)}.$$

Lemma 9. *Let* $\mathbb{K} = K_k(Z, w)$*, for* $k \geq 2$*, with* $Z = (\delta I + A)^{-1}$*. Then for* $j = 0, 1$ *and for any* $p_{k-1} \in \Pi_{k-1}$ *it is*

$$D(\xi)w = D(\xi)\frac{p_{k-1}(Z)A^j w}{\xi^j p_{k-1}((\xi+\delta)^{-1})}.$$

Proof. Use (A.2) with $b = p_{k-2}(Z)Zw$ for any $p_{k-2} \in \Pi_{k-2}$ and the identity $AZ = (I - \delta Z)$. □

Here and for the sequel we define

$$\Phi(\varkappa) = \varkappa + \sqrt{\varkappa^2 - 1}, \quad \varkappa \geq 1.$$

The following two lemmas follow by a result given in [51, Theorem 1].

Lemma 10. *Under our assumptions on A, there exists $p_k \in \Pi_k$ such that*

$$\left\| \frac{p_k(Z)}{p_k((\xi+\delta)^{-1})} \right\| \leq \frac{2}{\Phi(\omega)^k}, \quad \omega \equiv \omega(\xi) = \frac{\delta + a + |\xi - a|}{|\xi + \delta|}.$$

Lemma 11. *Let the spectrum of A be contained in the interval $[a, b]$. For any $\lambda \notin [a, b]$ there exists $p_k \in \Pi_k$ such that*

$$\left\| \frac{p_k(A)}{p_k(\lambda)} \right\| \leq \frac{2}{\Phi(\varkappa(\lambda))^k}, \quad \varkappa(\lambda) = \frac{|b - \lambda| + |a - \lambda|}{b - a}.$$

Lemma 12. *For any $\nu > 1$, $\sigma > 1$, $c \geq 1$ and $d \geq 1$ it is*

$$\int_1^{+\infty} r^{-\nu} \exp\left(\frac{-\sigma}{1 + r^c d}\right) dr \leq C \left(\frac{\sigma}{d}\right)^{\frac{1-\nu}{c}}.$$

Proof. The proof follows, after simple computation, by applying formulas 13.2.1 and 13.1.5 in [52]. □

Lemma 13. *There exists a constant C such that for every symmetric and positive definite matrix L and for any vector w, it is*

$$\int_{-\infty}^{\infty} \left\| ((1 + is)I \pm iL)^{-1} w \right\|^2 ds \leq C \left\| w \right\|^2.$$

Proof. The result follows from Plancharel's Theorem (see e.g. [53]). □

Proof of Proposition 2. For $\frac{1}{2} < \alpha < 1$, let $\varepsilon > 0$ and $\mu = (1 + \alpha)\pi/4$. We observe that, by the representation (6) and owing to Cauchy theorem, $y_\alpha(t)$ can be expressed as

$$y_\alpha(t) = -\frac{1}{2\alpha\pi} \int_{\Gamma(\varepsilon,\mu)} \exp(t\lambda^{\frac{1}{\alpha}})(i\lambda I - A)^{-1} v \, d\lambda, \tag{A.3}$$

where $\Gamma(\varepsilon, \mu) = \Gamma_1(\varepsilon, \mu) \cup \Gamma_2(\varepsilon, \mu)$ with $\Gamma_1(\varepsilon, \mu)$ the vertical segment

$$\Gamma_1(\varepsilon, \mu) = \{\lambda : \lambda = \varepsilon + i\rho, \quad -\varepsilon \tan \mu \leq \rho \leq \varepsilon \tan \mu\}$$

and

$$\Gamma_2(\varepsilon, \mu) = \{\lambda : \lambda = \varepsilon r \exp(\pm i\mu), \quad r \geq 1/\cos \mu\}.$$

Moreover, for convenience we write

$$\|y_\alpha(t) - \overline{y}_\alpha(t)\| \leq I_1 + I_2, \tag{A.4}$$

where by (A.3) we set

$$I_k = \frac{1}{2\alpha\pi}\left\|\int_{\Gamma_k(\varepsilon,\mu)} \exp(t\lambda^{\frac{1}{\alpha}})D(i\lambda)v d\lambda\right\|, \quad k=1,2,$$

and each integral represents the contribute of the corresponding part of the contour to the whole integral on $\Gamma(\varepsilon,\mu)$. Thanks to Lemma 9, with $j=1$,

$$I_k = \frac{1}{2\alpha\pi}\left\|\int_{\Gamma_k(\varepsilon,\mu)} \frac{\exp(t\lambda^{\frac{1}{\alpha}})D(i\lambda)p_m(Z)Av}{\lambda\, p_m((i\lambda+\delta)^{-1})}d\lambda\right\|, \quad k=1,2,$$

for any $p_m \in \Pi_m$. We note that (A.4) can be extended, by letting $\alpha \to 1$, since the well-known representation (see [53, p. 234])

$$y_1(t) = \frac{1}{2\pi i}\lim_{n\to+\infty}\int_{\varepsilon-in}^{\varepsilon+in} \exp(t\lambda)(\lambda I + iA)^{-1}v d\lambda.$$

Let us set $\varepsilon=\delta$. For I_1 observe that $|\exp(t\lambda^{\frac{1}{\alpha}})| = \exp(t\delta^{\frac{1}{\alpha}}(1+s^2)^{\frac{1}{2\alpha}}\cos(\alpha^{-1}\arctan s))$, where $s=\rho/\delta$. Since $(1+s^2)^{\frac{1}{2\alpha}}\cos(\alpha^{-1}\arctan s) \le 1$, we have

$$\left|\exp(t\lambda^{\frac{1}{\alpha}})\right| \le \exp\left(t\delta^{\frac{1}{\alpha}}\right) \tag{A.5}$$

and, moreover, by Lemma 13 it is

$$\int_{-\tan\mu}^{\tan\mu} \|D(1+is)w\|^2\, ds \le C\,\|w\|^2\,. \tag{A.6}$$

In order to apply Lemma 10, we observe that

$$\omega(i\lambda) = \frac{\delta + a + |i\lambda - a|}{|i\lambda+\delta|} \ge \frac{\delta+|\lambda|}{|i\lambda+\delta|}$$

and therefore, for any $\lambda \in \Gamma_1(\delta,\mu)$ we get

$$\omega(i\lambda) \ge \omega^*(s) = \frac{1+\sqrt{1+s^2}}{\sqrt{1+(s+1)^2}} \tag{A.7}$$

and hence $\Phi(\omega(i\lambda))^{-1} \le q = \Phi(\widetilde{\omega})^{-1}$. Accordingly, by Lemma 10, and taking into account of (A.6), (A.5) and the Schwarz's inequality, we obtain

$$I_1 \le \frac{C\exp(t\delta^{\frac{1}{\alpha}})q^{-m}\,\|Av\|}{\delta}\left(\int_0^{\tan\mu}(1+s^2)^{-1}ds\right)^{\frac{1}{2}}$$

and hence we can conclude that

$$I_1 \leq \frac{C\exp(t\delta^{\frac{1}{\alpha}})\,\|Av\|\,q^m}{\delta}. \tag{A.8}$$

Now let us consider $\lambda \in \Gamma_2(\delta,\mu)$. As $\varepsilon = \delta$, we get $\omega(i\lambda) \geq \omega^*(r)$, where $\omega^*(r) = (1+r)/(\sqrt{r^2+1+2r\sin\mu})$, for $r \geq 1/\cos\mu$. Thus

$$\Phi(\omega(i\lambda)) \geq \Phi(\omega^*(r)) = \frac{1+r+\sqrt{2r(1-\sin\mu)}}{\sqrt{r^2+1+2r\sin\mu}}$$

and by a simple computation one verifies that $\Phi(\omega^*(r))^2 \geq 1+2r^{-\frac{1}{2}}\cos\mu$ and hence

$$\Phi(\omega^*(r))^{-2} \leq \exp\left(-\frac{2\cos\mu}{\sqrt{r}}\right). \tag{A.9}$$

Now we claim that for every vector w it holds that

$$\int_{\frac{1}{\cos\mu}}^{\infty} \left\|(r\exp(i\mu)I - i\delta^{-1}A)^{-1}w\right\|^2 dr \leq C\,\|w\|^2. \tag{A.10}$$

Indeed, for $r \geq 1/\cos\mu$, first set $\eta = r\sin\mu$. From

$$\begin{aligned}
&((r\cos\mu+i\eta)I - i\delta^{-1}A)^{-1} - ((1+i\eta)I - i\delta^{-1}A)^{-1} \\
&\quad = \quad ((r\cos\mu+i\eta)I - i\delta^{-1}A)^{-1}(1-r\cos\mu)((1+i\eta)I - i\delta^{-1}A)^{-1},
\end{aligned}$$

and since $\left\|((r\cos\mu+i\eta)I + i\delta^{-1}A)^{-1}\right\| \leq 1/(r\cos\mu)$, we easily obtain

$$\left\|((r\cos\mu+i\eta)I - i\delta^{-1}A)^{-1}\right\| \leq (2-\frac{1}{r\cos\mu})\left\|((1+i\eta)I - i\delta^{-1}A)^{-1}\right\|.$$

By this inequality we get

$$\int_{\frac{1}{\cos\mu}}^{\infty} \left\|(ir\exp(i\mu)I + \delta^{-1}A)^{-1}w\right\|^2 dr \leq C\int_{\tan\mu}^{\infty} \left\|((1+i\eta)I - i\delta^{-1}A)^{-1}w\right\|^2 d\eta$$

and (A.10) follows from Lemma 13. A similar inequality clearly holds by replacing A with $\overline{A}$ as well as by replacing μ with $-\mu$. Therefore we deduce that for $\lambda \in \Gamma_2(\delta,\mu)$ it is

$$\int_{\frac{1}{\cos\mu}}^{\infty} \|D(i\lambda)w\|^2\,dr \leq C\delta^{-2}\,\|w\|^2. \tag{A.11}$$

Since $\cos(\mu/\alpha) < 0$, by applying Lemma 10 and the Schwarz's inequality, from (A.9) and (A.11)) we get

$$I_2 \leq C\frac{\|Av\|}{\delta}\left(\int_{\frac{1}{\cos\mu}}^{\infty} r^{-2}\exp\left(-f(r)\right)dr\right)^{\frac{1}{2}}. \tag{A.12}$$

By a simple analysis of the function $f(r)$ one finds that, for $r \geq 1$, $f(r) \geq f(r_m)$. Therefore, from (A.12) we get

$$I_2 \leq C\frac{\|Av\|}{\delta}\exp\left(-\frac{f(r_m)}{2}\right)\sqrt{\cos\mu} \tag{A.13}$$

and after combining this inequality with (A.8) and (A.14), by (A.3) it is possible to prove (11).

In order to study what happens as $\alpha \to 1$, let us reconsider I_1. We observe that by referring to (A.7), it is possible to observe that when $s \leq 1$ it follows $\Phi(\omega^*(s))^{-1} \leq \bar{q}$. Moreover, it is not difficult to see that, for $s \geq 1$ we have $\Phi(\omega^*(s)) \geq \sqrt{1+s^{-3/2}}$ and hence $\Phi(\omega^*(s))^{-2} \leq \exp(-1/(1+s^{3/2}))$. By this bound, and by arguing as before, we obtain

$$I_1 \leq \frac{C\exp(t\delta^{\frac{1}{\alpha}})\,\|Av\|}{\delta}\left[\bar{q}^{m-1} + \left(\int_1^{\tan\mu}(1+s^2)^{-1}\exp\left(\frac{-m}{1+s^{3/2}}\right)ds)\right)^{\frac{1}{2}}\right].$$

We now apply Lemma 12 to obtain

$$\int_1^{+\infty}(1+s^2)^{-1}\exp\left(\frac{-m}{1+s^{3/2}}\right)ds \leq Cm^{-\frac{2}{3}}$$

and therefore we get

$$I_1 \leq \frac{C\exp(t\delta^{\frac{1}{\alpha}})\,\|Av\|}{\delta}(\bar{q}^m + m^{-\frac{1}{3}}) \tag{A.14}$$

and now (12) follows from (A.14) and (A.13), since $\mu = (1+\alpha)\pi/4$. □

Proof of Proposition 3. Let us start again from formulas (A.3) and (A.4). By employing Lemma 8 we easily obtain

$$I_k = \frac{1}{2\alpha\pi}\left\|\int_{\Gamma_k(\varepsilon,\mu)}\frac{\exp(t\lambda^{\frac{1}{\alpha}})}{\lambda^m}D(i\lambda)A^m v d\lambda\right\|, \quad k = 1, 2. \tag{A.15}$$

Let $\lambda \in \Gamma_1(\varepsilon, \mu)$, then (A.5) holds with $\delta = \varepsilon$ and, moreover, $\|D(i\lambda)\| \leq 2/\varepsilon$. Therefore, setting $s = \rho/\varepsilon$, we get

$$I_1 \leq C \frac{\exp(t\varepsilon^{\frac{1}{\alpha}})\,\|A^m v\|}{\varepsilon^m} \int_0^{\tan\mu} (1+s^2)^{-\frac{m}{2}}\,ds. \tag{A.16}$$

Now let $\lambda \in \Gamma_2(\varepsilon, \mu)$. We have $\|D(i\lambda)\| \leq 2/(\varepsilon r \cos\mu)$ and $|\exp(t\lambda^{\frac{1}{\alpha}})| \leq \exp(-2t(\varepsilon r)^{\frac{1}{\alpha}}\,|\cos(\mu/\alpha)|)$ and, as a consequence,

$$I_2 \leq \frac{C}{\varepsilon^m \cos\mu} \int_{\frac{1}{\cos\mu}}^{+\infty} \exp\left(-t(\varepsilon r)^{\frac{1}{\alpha}} \left|\cos\frac{\mu}{\alpha}\right|\right) r^{-m-1} dr \leq C \frac{(\cos\mu)^{m-1}}{m\varepsilon^m}. \tag{A.17}$$

Therefore, after inserting (A.16) and (A.17) in (A.15) we get

$$\|y_\alpha(t) - \overline{y}_\alpha(t)\| \leq C \frac{\|A^m v\|}{\varepsilon^m} \exp(t\varepsilon^{\frac{1}{\alpha}})$$

and the proof follows after choosing $\varepsilon = (\alpha m/t)^\alpha$ which minimizes $\exp(t\varepsilon^{\frac{1}{\alpha}})/\varepsilon^m$. □

Proof of Proposition 4. Let us set $\gamma = 1/\alpha$. Consider the positively oriented (counterclockwise) contour G consisting of the following parts:

$$\begin{aligned} G_{2+} &= \left\{\lambda = \delta r \exp(i\tfrac{\pi}{3r^\gamma}), \quad 1 \leq r < +\infty\right\} \\ G_1 &= \left\{\lambda = \tfrac{\delta}{2}(1+i\rho), \quad -\sqrt{3} \leq \rho \leq \sqrt{3}\right\} \\ G_{2-} &= \left\{\lambda = \delta r \exp(-i\tfrac{\pi}{3r^\gamma}), \quad 1 \leq r < +\infty\right\} \end{aligned}$$

and, for the sake of simplicity, we set $G_2 = G_{2+} \cup G_{2-}$. Let $\delta = a$. For any $t > 0$, the function $\exp(-it\lambda^\gamma)/\lambda$ is analytic in the convex set surrounded by G and, by the Dunford–Taylor representation theorem [54, p. 601], we realize that

$$w_\alpha(t) - \overline{w}_\alpha(t) = \frac{1}{2\pi\alpha i} \int_G \frac{\exp(-it\lambda^\gamma)}{\lambda} D(\lambda) A v\, d\lambda$$

so that $\|w_\alpha(t) - \overline{w}_\alpha(t)\| \leq I_1 + I_2$, where

$$I_k = \frac{1}{2\alpha\pi} \left\| \int_{G_k} \frac{\exp(-it\lambda^\gamma)}{\lambda} D(\lambda) A v\, d\lambda \right\|, \quad k = 1, 2.$$

By exploiting Lemma 9 we get for any $p_m \in \Pi_m$,

$$I_k = \frac{1}{2\pi\alpha} \left\| \int_{G_k} \frac{\exp(-it\lambda^\gamma)}{\lambda^2} \frac{D(\lambda) p_m(Z) A^2 v}{p_m((\lambda+\delta)^{-1})}\, d\lambda \right\|, \quad k = 1, 2. \tag{A.18}$$

When $\lambda \in G_1$ we easily verify that

$$\left|\frac{\exp(-it\lambda^\gamma)}{\lambda^2}\right| \le \frac{4}{a^2(1+\rho^2)} \exp\left(t\frac{\pi}{3\alpha}a^\gamma\right) \tag{A.19}$$

and, moreover, referring to (A.1), we find

$$\|D(\lambda)\| \le \frac{4}{a}. \tag{A.20}$$

Now let us apply Lemma 10. For $\lambda = \frac{a}{2}(1 \pm i\,|\rho|)$, it is easy to verify that, for any $0 \le |\rho| \le \sqrt{3}$, it holds that $\omega(\lambda) \ge (2\delta + 3a)/(2\delta + a)$ and, since $\delta = a$, it is $\Phi(\omega(\lambda))^{-1} \le 1/3$. Then, taking into account of all the previous inequalities, we obtain

$$I_1 \le \bar{C}\frac{\|A^2 v\| \exp\left(t\frac{\pi}{3\alpha}a^\gamma\right)}{a^2}3^{-m}\int_0^{\sqrt{3}} \frac{1}{1+\rho^2}\,d\rho = C\frac{\|A^2 v\| \exp\left(t\frac{\pi}{3\alpha}a^\gamma\right)}{a^2}3^{-m}. \tag{A.21}$$

We proceed in an analogous way for $\lambda \in G_2$. At first one verifies that

$$|\exp(-it\lambda^\gamma)| \le \exp\left(t\frac{\pi a^\gamma}{3\alpha}\right), \tag{A.22}$$

$$|d\lambda| \le a\left(\sqrt{1+\frac{\pi^2}{9}r^{-2\gamma}}\right) dr \tag{A.23}$$

and

$$\|D(\lambda)\| \le \frac{2}{ar\sin\frac{\pi}{3r^\gamma}} \le \frac{1}{a}Cr^{\gamma-1}. \tag{A.24}$$

In order to apply Lemma 10, we observe that $\omega(\lambda) \ge \omega^*(r)$, where

$$\omega^*(r) = \frac{1+r}{\sqrt{r^2+1+2r\cos\frac{\pi}{3r^\gamma}}}$$

and hence, by the above inequalities, we obtain

$$I_2 \le C\frac{\|A^2 v\|}{a^2}\int_1^\infty r^{-3+\gamma}\Phi(\omega^*(r))^{-m}dr. \tag{A.25}$$

Since

$$\Phi(\omega^*(r)) = \frac{1+r+\sqrt{2r(1-\cos\frac{\pi}{3r^\gamma})}}{\sqrt{r^2+1+2r\cos\frac{\pi}{3r^\gamma}}},$$

it is not difficult to see that

$$\Phi(\omega^*(r))^2 \geq 1 + \sqrt{\frac{1}{r}\left(1 - \cos\frac{\pi}{3r^\gamma}\right)} \geq 1 + \frac{1}{2} r^{-\frac{1}{2}-\gamma}$$

and, hence, $\Phi(\omega^*(r))^{-2} \leq \exp(-(1+2r^{\frac{1}{2}+\gamma})^{-1})$. Therefore we get

$$\int_1^\infty r^{-3+\gamma}\Phi(\omega^*(r))^{-m} dr \leq \int_1^\infty r^{-3+\gamma} \exp\left(\frac{-m}{2\left(1+2r^{\frac{\alpha+2}{2\alpha}}\right)}\right) dr$$

thanks to which Lemma 12 leads to

$$\int_1^\infty r^{-3+\gamma}\Phi(\omega(r))^{-(m-1)} \leq C\left(\frac{4}{m}\right)^{\frac{2(2\alpha-1)}{\alpha+2}}$$

and the result follows from Equations (A.18), (A.21) and (A.25). □

Proof of Proposition 5. Let us consider again the contour G previously introduced and, owing to Lemma 8, we easily realize that $\|w_\alpha(t) - \overline{w}_\alpha(t)\| \leq I_1 + I_2$, where for any $p_m \in \Pi_m$ it is

$$I_k = \frac{1}{2\alpha\pi}\left\|\int_{G_k} \frac{\exp(it\lambda^\gamma)}{\lambda^2}\frac{D(\lambda)p_m(A)A^2 v}{p_m(\lambda)} d\lambda\right\|, \quad k = 1, 2.$$

We observe that, for $\lambda \in G_1$

$$\varkappa(\lambda) = \frac{|b-\lambda| + |\lambda - a|}{b-a} \geq \frac{b}{b-a}$$

and, accordingly, by using Lemma 11, (A.19) and (A.20), we obtain

$$I_1 \leq C\frac{\|A^2 v\|}{a^2}\exp\left(t\frac{\pi a^\gamma}{3\alpha}\right)\Phi\left(\frac{R+1}{R}\right)^{-m}.$$

Since, for $x \geq 0$, it holds that

$$\Phi(1+x)^{-n} = \mathcal{O}(\exp(-n\sqrt{2x})), \tag{A.26}$$

we get

$$I_1 \leq C\frac{\|A^2 v\|}{a^2}\exp\left(\frac{t\pi a^\gamma}{3\alpha}\right)\exp\left(-\frac{m\sqrt{2}}{\sqrt{R}}\right). \tag{A.27}$$

For $\lambda \in G_2$ we observe that

$$\begin{aligned} \varkappa(\lambda) &= \frac{\sqrt{(R+1)^2 + r^2 - 2(R+1)r\cos\frac{\pi}{3r^\gamma}} + \sqrt{1 + r^2 - 2r\cos\frac{\pi}{3r^\gamma}}}{R} \\ &\geq 1 + \frac{r}{R}\left(1 - \cos\frac{\pi}{3r^\gamma}\right) \end{aligned}$$

and, since $r(1 - \cos\frac{\pi}{3r^\gamma}) \geq r^{1-2\gamma}/4$, by (A.26) it follows

$$\Phi(\varkappa(\lambda))^{-m} \leq C \exp\left(\frac{-mr^{\frac{1-2\gamma}{2}}}{\sqrt{2R}}\right).$$

Therefore, by (A.22), (A.23), (A.24) and Lemma 11, it holds that

$$I_2 \leq C\frac{\|A^2v\|}{a^2}\exp\left(\frac{t\pi a^\gamma}{3\alpha}\right)\int_1^{+\infty} r^{-3+\gamma}\exp\left(\frac{-m}{\sqrt{2R}r^{\frac{2\gamma-1}{2}}}\right)dr$$

and by Lemma 12 we obtain the inequality

$$I_2 \leq C\frac{\|A^2v\|}{a^2}\exp\left(t\frac{\pi a^\gamma}{3\alpha}\right)\left(\frac{\sqrt{2R}}{m}\right)^{\frac{2(2\alpha-1)}{2-\alpha}}$$

which, together with (A.27), allows to prove the result. □

Proof of Proposition 6. Referring to (7) let us consider the contour $Q = Q(\frac{a}{2}, \alpha\pi)$, $\frac{1}{2} < \alpha < 1$. From (6) and (A.1) we have

$$\|u_\alpha(t) - \overline{u}_\alpha(t)\| \leq I_1 + I_2, \tag{A.28}$$

where

$$I_k = \frac{1}{2\alpha\pi}\left\|\int_{Q_k}\exp(-it\lambda^{\frac{1}{\alpha}})D(i^\alpha\lambda)vd\lambda\right\|, \quad k = 1, 2,$$

with $Q_1 = \left\{\lambda \,:\, \lambda = \frac{a}{2}\exp(i\arg\lambda),\, -\mu \leq \arg\lambda < \mu\right\}$ and $Q_2 = Q\backslash Q_1$. Then, by Lemma 9, for any $p_m \in \Pi_m$ it is

$$I_k = \frac{1}{2\alpha\pi}\left\|\int_{Q_k}\frac{\exp(t\lambda^{\frac{1}{\alpha}})}{\lambda}\frac{D(i^\alpha\lambda)p_m(Z)Av}{p_m((i^\alpha\lambda + \delta)^{-1})}d\lambda\right\|, \quad k = 1, 2. \tag{A.29}$$

For $\lambda \in Q_1$ we get

$$\|D(i^\alpha\lambda)\| \leq \frac{4}{a}. \tag{A.30}$$

We consider now

$$\omega(i^\alpha\lambda) = \frac{\delta + a + |i^\alpha\lambda - a|}{|i^\alpha\lambda + \delta|}$$

and for any $\lambda \in Q_1$ it is easy to verify that $\omega(i^\alpha\lambda) \geq (2\delta + 3a)/(2\delta + a)$ and thus, by using $\delta = a$, we have $\Phi(\omega(i^\alpha\lambda))^{-1} \leq 1/3$. Therefore, by Lemma 10 and from (A.29) we easily obtain

$$I_1 \leq C\frac{\|Av\|}{a}\exp\left(ta^{\frac{1}{\alpha}}\right)3^{-m}. \tag{A.31}$$

Let $\lambda \in Q_2$, namely $\lambda = ar\exp(\pm i\mu)$, for $\frac{1}{2} < r < \infty$. We realize that

$$\omega(i^\alpha\lambda) \geq \frac{1+r}{\sqrt{r^2 + 1 + 2r\cos(\pm\mu + \alpha\frac{\pi}{2})}}$$

and, after observing that $\cos(\pm\mu + \alpha\frac{\pi}{2}) \leq 1/\sqrt{2}$, we get

$$\omega(i^\alpha\lambda) \geq \omega^*(r) = \frac{1+r}{\sqrt{r^2+1+\sqrt{2}r}}.$$

Therefore, since $\|D(i^\alpha\lambda)\| \leq C/(ar)$, by applying Lemmas 9 and 10 we obtain

$$I_2 \leq C\frac{\|Av\|}{a}\int_1^\infty \frac{\exp(-t(ar)^{\frac{1}{\alpha}})}{r^2}\Phi(\omega^*(r))^{-m}dr, \tag{A.32}$$

where

$$\Phi(\omega^*(r)) = \frac{1 + r + \sqrt{(2-\sqrt{2})r}}{\sqrt{r^2+1+\sqrt{2}r}}.$$

One can see that $\Phi(\omega^*(r))^2 \geq 1+1/(2r)$ and hence we find $\Phi(\omega^*(r))^{-2} \leq \exp(-1/(1+2r)) \leq \exp(-1/(4r))$. Therefore, from (A.32) it follows that

$$I_2 \leq C\frac{\|Av\|}{a}\int_{1/2}^\infty \frac{\exp(-f(r))}{r^2}dr.$$

A simple analysis shows that $f(r) \geq f(r_m)$ and we can conclude that $I_2 \leq C\frac{\|Av\|}{a}\exp(-f(r_m))$ and the result follows by collecting the above inequality with (A.31). $\square$

Proof of Proposition 7. Consider again the contour $Q = Q(\frac{a}{2}, \alpha\pi)$ and formula (A.28), where, owing to Lemma 8, it holds

$$I_k = \frac{1}{2\alpha\pi} \left\| \int_{Q_k} \frac{\exp(t\lambda^{\frac{1}{\alpha}})}{\lambda} \frac{D(i^\alpha\lambda)p_m(A)Av}{p_m(i^\alpha\lambda)} d\lambda \right\|, \quad k = 1, 2,$$

for any $p_m \in \Pi_m$. Referring to Lemma 11, we observe that for $\lambda \in Q_1$ it is $\varkappa(i^\alpha\lambda) \geq 1 + 1/R$. Therefore, by recalling (A.26), we get $\Phi(\varkappa(i^\alpha\lambda))^{-m} \leq \mathcal{O}\left(\exp(-m\sqrt{2/R})\right)$ and thus, by (A.30) and Lemma 11, it is

$$I_1 \leq C\frac{\|Av\|}{a} \exp\left(t\left(\frac{a}{2}\right)^{\frac{1}{\alpha}} - m\sqrt{2/R}\right). \tag{A.33}$$

Now consider $\lambda \in Q_2$. For the corresponding $\varkappa(i^\alpha\lambda)$ one finds

$$\varkappa(i^\alpha\lambda) = \frac{\left|b - ar\exp(-i\alpha\frac{\pi}{2})\right| + a\left|1 - r\exp(-i\alpha\frac{\pi}{2})\right|}{b-a}$$

and, since $\cos(-\alpha\pi/2) \leq 1/\sqrt{2}$, it is

$$\varkappa(i^\alpha\lambda) \geq \frac{\sqrt{(R+1)^2 + r^2 - \sqrt{2}(R+1)r} + \sqrt{1 + r^2 - \sqrt{2}r}}{R}. \tag{A.34}$$

By a simple analysis one finds that the right-hand side of (A.34) attains the minimum at $r = \sqrt{2}(R+1)/(R+2)$ and, by a simple computation, we obtain $\varkappa(i^\alpha\lambda) \geq 1 + 1/R$ and therefore, thanks to the Equation (A.26), it is $\Phi(\varkappa(i^\alpha\lambda))^{-m} \leq \mathcal{O}\left(\exp(-m\sqrt{2/R})\right)$.

Thus, since $\|D(i^\alpha\lambda)\| \leq C/(ar)$ and $\left|\exp(-t\lambda^{\frac{1}{\alpha}})\right| \leq \exp(-t(ar)^{\frac{1}{\alpha}})$, by Lemmas 8 and Lemma 11, we have

$$I_2 \leq \frac{C\,\|Av\|}{a} \int_1^{+\infty} \frac{\exp(-t(ar)^{\frac{1}{\alpha}} - m\sqrt{2/R})}{r^2} dr,$$

and the result follows from formula (A.28) after applying the above inequality and equation (A.33). □

References

[1] E. Schrödinger, An undulatory theory of the mechanics of atoms and molecules, Phys. Rev. 28 (1926) 1049–1070.

[2] D. Baleanu, K. Diethelm, E. Scalas, J. J. Trujillo, Fractional calculus. Models and numerical methods, Vol. 3 of Series on Complexity, Nonlinearity and Chaos, World Scientific Publishing Co. Pte. Ltd., Hackensack, NJ, 2012.

[3] R. Caponetto, G. Dongola, L. Fortuna, I. Petráš, Fractional Order Systems: Modeling and Control Applications, Vol. 72 of Series on Nonlinear Science, Series A, World Scientific, Singapore, 2010.

[4] K. Diethelm, The analysis of fractional differential equations, Vol. 2004 of Lecture Notes in Mathematics, Springer-Verlag, Berlin, 2010.

[5] R. Herrmann, Fractional Calculus: An Introduction for Physicists, World Scientific, 2011.

[6] F. Mainardi, Fractional calculus and waves in linear viscoelasticity, Imperial College Press, London, 2010.

[7] I. Podlubny, Fractional differential equations, Vol. 198 of Mathematics in Science and Engineering, Academic Press Inc., San Diego, CA, 1999.

[8] N. Laskin, Fractional quantum mechanics and Lévy path integrals, Physics Letters A 268 (4-6) (2000) 298–305.

[9] E. Scalas, D. Baleanu, F. Mainardi, A. Mura, Fractional calculus and the Schrödinger equation, IFAC Proceedings Volumes (IFAC-PapersOnline) 2 (PART 1) (2006) 234–237.

[10] S. I. Muslih, O. P. Agrawal, D. Baleanu, A fractional Schrödinger equation and its solution, Int. J. of Theoretical Physics 49 (8) (2010) 1746–1752.

[11] E. Capelas de Oliveira, J. Vaz Jr., Tunneling in fractional quantum mechanics, Journal of Physics A: Mathematical and Theoretical 44 (18) (2011) 185303.

[12] Y. Luchko, Fractional Schrödinger equation for a particle moving in a potential well, J. Math. Phys. 54 (1) (2013) 012111, 10.

[13] B. Al-Saqabi, L. Boyadjiev, Y. Luchko, Comments on employing the Riesz-Feller derivative in the Schrödinger equation, Eur. Phys. J. Special Topics 222 (8) (2013) 1779–1794.

[14] M. Naber, Time fractional Schrödinger equation, J. Math. Phys. 45 (8) (2004) 3339–3352.

[15] A. Ashyralyev, B. Hicdurmaz, On the numerical solution of fractional Schrödinger differential equations with the Dirichlet condition, Int. J. Comput. Math. 89 (13-14) (2012) 1927–1936.

[16] P. Rozmej, B. Bandrowski, On fractional Schrödinger equation, Comput. Methods Sci. Technol 16 (2010) 191–194.

[17] E. Gallopoulos, Y. Saad, Efficient solution of parabolic equations by Krylov approximation methods, SIAM J. Sci. Statist. Comput. 13 (5) (1992) 1236–1264.

[18] L. Lopez, V. Simoncini, Preserving geometric properties of the exponential matrix by block Krylov subspace methods, BIT 46 (4) (2006) 813–830.

[19] I. Moret, P. Novati, On the convergence of Krylov subspace methods for matrix Mittag–Leffler functions, SIAM J. Numer. Anal. 49 (5) (2011) 2144–2164.

[20] M. Hochbruck, A. Ostermann, Exponential integrators, Acta Numer. 19 (2010) 209–286.

[21] R. Garrappa, M. Popolizio, Generalized exponential time differencing methods for fractional order problems, Comput. Math. Appl. 62 (3) (2011) 876–890.

[22] R. Garrappa, M. Popolizio, On accurate product integration rules for linear fractional differential equations, J. Comput. Appl. Math. 235 (5) (2011) 1085–1097.

[23] R. Garrappa, M. Popolizio, On the use of matrix functions for fractional partial differential equations, Math. Comput. Simulation 81 (5) (2011) 1045–1056.

[24] I. Moret, M. Popolizio, The restarted shift-and-invert Krylov method for matrix functions, Numer. Linear Algebra Appl. 21 (1) (2014) 68–80.

[25] I. Moret, A note on Krylov methods for fractional evolution problems, Numer. Funct. Anal. Optim. 34 (5) (2013) 539–556.

[26] I. Moret, Shift-and-invert Krylov methods for time-fractional wave equations, Numerical Functional Analysis and Optimization-doi:10.1080/01630563.2014.908209.

[27] M. Popolizio, A matrix approach for partial differential equations with Riesz space fractional derivatives, Eur. Phys. J. Special Topics 222 (8) (2013) 1975–1985.

[28] T. Kato, Perturbation theory for linear operators, Classics in Mathematics, Springer-Verlag, Berlin, 1995, reprint of the 1980 edition.

[29] B. N. Narahari Achar, B. T. Yale, J. W. Hanneken, Time fractional Schrödinger equation revisited, Advances in Mathematical Physics 2013 (290216) (2013) 1.

[30] S. Ş. Bayın, Time fractional Schrödinger equation: Fox's H-functions and the effective potential, J. Math. Phys. 54 (1) (2013) 012103, 18.

[31] A. A. Kilbas, H. M. Srivastava, J. J. Trujillo, Theory and applications of fractional differential equations, Vol. 204 of North-Holland Mathematics Studies, Elsevier Science B.V., Amsterdam, 2006.

[32] A. Erdélyi, W. Magnus, F. Oberhettinger, F. G. Tricomi, Higher transcendental functions. Vol. III, Robert E. Krieger Publishing Co., Inc., Melbourne, Fla., 1981.

[33] M. M. Džrbašyan, On the integral representation of functions continuous on several rays (generalization of the Fourier integral), Izv. Akad. Nauk SSSR. Ser. Mat. 18 (1954) 427–448.

[34] R. Gorenflo, J. Loutchko, Y. Luchko, Computation of the Mittag-Leffler function $E_{\alpha,\beta}(z)$ and its derivative, Fract. Calc. Appl. Anal. 5 (4) (2002) 491–518, dedicated to the 60th anniversary of Prof. Francesco Mainardi.

[35] H. Seybold, R. Hilfer, Numerical algorithm for calculating the generalized Mittag-Leffler function, SIAM J. Numer. Anal. 47 (1) (2008/09) 69–88.

[36] R. Gorenflo, F. Mainardi, Fractional calculus: integral and differential equations of fractional order, in: Fractals and fractional calculus in continuum mechanics (Udine, 1996), Vol. 378 of CISM Courses and Lectures, Springer, Vienna, 1997, pp. 223–276.

[37] K. S. Miller, S. G. Samko, Completely monotonic functions, Integral Transform. Spec. Funct. 12 (4) (2001) 389–402.

[38] E. Capelas de Oliveira, F. Mainardi, J. Vaz Jr., Models based on Mittag–Leffler functions for anomalous relaxation in dielectrics, Eur. Phys. J. Special Topics 193 (2011) 161–171.

[39] W. R. Schneider, Completely monotone generalized Mittag-Leffler functions, Exposition. Math. 14 (1) (1996) 3–16.

[40] F. Mainardi, R. Gorenflo, On Mittag-Leffler-type functions in fractional evolution processes, J. Comput. Appl. Math. 118 (1-2) (2000) 283–299.

[41] C. Moler, C. Van Loan, Nineteen dubious ways to compute the exponential of a matrix, SIAM Rev. 20 (4) (1978) 801–836.

[42] C. Moler, C. Van Loan, Nineteen dubious ways to compute the exponential of a matrix, twenty-five years later, SIAM Rev. 45 (1) (2003) 3–49.

[43] C. Lubich, From quantum to classical molecular dynamics: reduced models and numerical analysis, Zurich Lectures in Advanced Mathematics, European Mathematical Society (EMS), Zürich, 2008.

[44] T. J. Park, J. C. Light, Unitary quantum time evolution by iterative Lanczos reduction, The Journal of Chemical Physics 85 (10) (1986) 5870–5876.

[45] R. Garrappa, M. Popolizio, Evaluation of generalized Mittag–Leffler functions on the real line, Advances in Computational Mathematics 39 (1) (2013) 205–225. doi:10.1007/s10444-012-9274-z.

[46] M. Popolizio, V. Simoncini, Acceleration techniques for approximating the matrix exponential operator, SIAM J. Matrix Anal. Appl. 30 (2) (2008) 657–683.

[47] N. J. Higham, Functions of matrices, Society for Industrial and Applied Mathematics (SIAM), Philadelphia, PA, 2008.

[48] N. J. Higham, L. Lin, A Schur-Padé algorithm for fractional powers of a matrix, SIAM J. Matrix Anal. Appl. 32 (3) (2011) 1056–1078.

[49] N. Hale, N. J. Higham, L. N. Trefethen, Computing $\mathbf{A}^{\alpha}$, $\log(\mathbf{A})$, and related matrix functions by contour integrals, SIAM J. Numer. Anal. 46 (5) (2008) 2505–2523.

[50] P. Novati, Numerical approximation to the fractional derivative operator, Numerische Mathematik 127 (3) (2014) 539–566.

[51] R. Freund, On conjugate gradient type methods and polynomial preconditioners for a class of complex non-Hermitian matrices, Numer. Math. 57 (3) (1990) 285–312.

[52] M. Abramowitz, I. A. Stegun, Handbook of mathematical functions with formulas, graphs, and mathematical tables, Vol. 55 of National Bureau of Standards Applied Mathematics Series, For sale by the Superintendent of Documents, U.S. Government Printing Office, Washington, D.C., 1964.

[53] K.-J. Engel, R. Nagel, One-parameter semigroups for linear evolution equations, Vol. 194 of Graduate Texts in Mathematics, Springer-Verlag, New York, 2000.

[54] N. Dunford, J. T. Schwartz, Linear Operators. I. General Theory, Interscience Publishers, Inc., New York; Interscience Publishers, Ltd., London, 1958.